Diffraction Study on the Atomic Structure and Phase Separation of Amorphous Ceramics in the Si−(B)−C−N System. 2. Si−B−C−N Ceramics

Jörg Haug,* Peter Lamparter, Markus Weinmann, and Fritz Aldinger

Max-Planck-Institut für Metallforschung, Heisenbergstrasse 3, D-70569 Stuttgart, Germany

Received June 2, 2003. Revised Manuscript Received August 25, 2003

The atomic structure and phase separation of amorphous Si−B−C−N ceramic powder samples obtained by thermolysis of boron-modified polysilazanes were investigated using X-ray and neutron diffraction in the wide-angle and small-angle scattering regimes. The short-range order of the Si−B−C−N ceramics corresponds to that of Si−C−N ceramics consisting of two separated amorphous phases: an amorphous graphite-like phase and amorphous $Si_{3+(1/4)x}N_{4-x}C_x$ ($x = 0-4$). The evaluation of the total pair correlation functions revealed that the boron atoms are bonded to nitrogen with B−N bond lengths typical for h-BN. These units are incorporated in the graphite-like phase not statistically, but within regions of BN-rings which are less extended than the regions formed by C-rings. X-ray diffraction phase analysis and small-angle scattering showed that the addition of up to 10 at. % of boron to Si−C−N ceramics significantly influences the high-temperature behavior of the ceramics: coarsening of the separated amorphous phases, the crystallization of Si_3N_4 and its decomposition are retarded, and evolution of a nanocrystalline SiC phase is observed.

1. Introduction

In Part I[1] of the present study we reported on the short- and medium-range order of precursor-derived Si−C−N ceramics covering a wide range of compositions. It has been shown that all the investigated ceramics are separated into an amorphous graphite-like phase and an amorphous silicon-containing phase in which the silicon atoms are tetrahedrally coordinated by nitrogen and carbon. Upon additional annealing, both phases coarsened.

Detailed investigations of the high-temperature behavior of such Si−C−N ceramics by means of thermogravimetric analysis showed that exceeding 1450−1500 °C in a nitrogen atmosphere, the thermal decomposition of the materials occurred because of a carbothermal reduction of Si−N units by carbon. In this reaction Si−C motifs form at the expense of Si−N bonds and nitrogen is released, resulting in a weight loss of the materials.[2−4]

During the last 10 years, quaternary precursor-derived Si−B−C−N ceramics gained in interest as they frequently resist thermal decomposition, even at temperatures exceeding 1800 °C.[5−9] In this context, two structurally very different precursor systems can be distinguished.

Jansen et al. described ammonolysis and aminolysis reactions of $Cl_3SiNHBCl_2$ (TADB) delivering precursors for $Si_3B_3N_7$ and $SiBN_3C$ ceramics, respectively. Structural features of $Si_3B_3N_7$ were investigated intensively by means of solid-state NMR spectroscopy,[10] transmission electron microscopy,[11] X-ray absorption near edge structure (XANES) measurements,[12] and X-ray as well as neutron diffraction.[13] It was concluded that $Si_3B_3N_7$ is composed of a three-dimensional random network bearing planar BN_3 units and distorted SiN_4 tetrahedra in boron-rich and silicon-rich regions, respectively,

* Corresponding author: Jörg Haug, Hahn Meitner Institut Berlin, Glienicker Strasse 100, D-14109 Berlin, Germany. E-mail: haug@hmi.de.

(1) Haug, J.; Lamparter, P.; Weinmann, M.; Aldinger, F. *Chem. Mater.* **2003**, *15*, .

(2) Bahloul, D.; Pereira, M.; Goursat, P. *J. Am. Ceram. Soc.* **1993**, *76*, 1163.

(3) Bill, J.; Aldinger, F. *Adv. Mater* **1995**, *7*, 775.

(4) Kroke, E.; Li, Y. L.; Konetschny, C.; Lecomte, E.; Fasel, C.; Riedel, R. *Mater. Sci. Eng.* **2000**, *R 26*, 97.

(5) (a) Jansen, M.; Baldus, H.-P. Ger. Offen. DE 410 71 08 A1, 1992. (b) Baldus, H.-P.; Jansen, M.; Wagner, O. *Key Eng. Mater.* **1994**, *89−91*, 75. (c) Baldus, H.-P.; Wagner, O.; Jansen, M. *Mater. Res. Soc. Symp. Proc.* **1992**, *271*, 821. (d) Jansen, M.; Jeschke, T. *Z. Anorg. Chem.* **1999**, *625*, 1957.

(6) (a) Baldus, H.-P.; Jansen, M. *Angew. Chem., Int. Ed. Engl.* **1997**, *36*, 329. (b) Jansen, M.; Jeschke, B.; Jeschke, T. *Struct. Bonding* **2002**, *101*, 137.

(7) (a) Riedel, R.; Kienzle, A.; Dressler, W.; Ruwisch, L.; Bill, J.; Aldinger, F. *Nature* **1996**, *382*, 796. (b) Riedel, R.; Kienzle, A.; Petzow, G.; Bruck, M.; Vaahs, T. Ger. Offen. DE 43 20 783 A1, 1994. (c) Kienzle, A. Ph.D. Thesis, Universität Stuttgart, Germany, 1994. (d) Riedel, R.; Bill, J.; Kienzle, A. *Appl. Organomet. Chem.* **1996**, *10*, 241.

(8) Weinmann, M.; Schuhmacher, J.; Kummer, H.; Prinz, S.; Peng, J.; Seifert, H. J.; Christ, M.; Müller, K.; Bill, J.; Aldinger, F. *Chem. Mater.* **2000**, *12*, 623.

(9) (a) Weinmann, M.; Zern, A.; Hörz, M.; Berger, F.; Müller, K.; Aldinger, F. *J. Met. Nano. Mater.* **2002**, *386−388*, 335. (ISSN: 1422-6375) (b) Weinmann, M.; Kamphowe, T. W.; Schuhmacher, J.; Müller, K.; Aldinger, F. *Chem. Mater.* **2000**, *12*, 2112. (c) Kamphowe, T. W.; Weinmann, M.; Bill, J.; Aldinger, F. *Silic. Ind.* **1998**, *63*, 159.

(10) (a) van Wüllen, L.; Müller, U.; Jansen, M. *Angew. Chem., Int. Ed.* **2000**, *39*, 2519. (b) Müller, U.; Hoffbauer, W.; Jansen, M. *Chem. Mater.* **2000**, *12*, 2341. (c) van Wüllen, L.; Müller, U.; Jansen, M. *Chem. Mater.* **2000**, *12*, 2347. (d) van Wüllen, L.; Jansen, M. J. *Mater. Chem.* **2001**, *11*, 223. (e) Jeschke, G.;. Kroschl, M.; Jansen, M. *J. Non-Cryst. Solids* **1999**, *260*, 216.

(11) Heinemann, D.; Assenmacher, W.; Mader, W.; Kroschl, M.; Jansen, M. *J. Mater. Res.* **1999**, *14*, 3746.

(12) Franke, R.; Bender, St.; Jungermann, H.; Kroschl, M.; Jansen, M. *J. Electron Spectrosc. Relat. Phenom.* **1999**, *101−103*, 641.

(13) Hagenmayer, R. M.; Müller, U.; Benmore, C. J.; Neuefeind, J.; Jansen, M. *J. Mater. Chem.* **1999**, *9*, 2865.

10.1021/cm031088t CCC: $27.50
Published on Web 12/11/2003

which are connected via nitrogen atoms. A similar structural constitution was suggested for $SiBN_3C$, which is comparably poor in carbon compared to the ceramics investigated in this paper. It was stated that $SiBN_3C$ is built up by BN_3, distorted SiN_4, NB_3, and mixed SiN_xC_y ($y < 4$) as well as NB_zSi_{3-z} units, whereas there was no hint for segregation of carbon-rich regions.

Riedel et al.[7] and our group synthesized Si−B−C−N−H polymers using different synthetic approaches. The precursors released carbon-rich ceramics after thermolysis with compositions located in the four-phase field $SiC/Si_3N_4/BN/C$.[8,9,14] Polymers were obtained by ammonolysis of $B(C_2H_4Si(CH_3)Cl_2)_3$[7] or $B(C_2H_4SiRCl_2)_3$ (R = H, Cl),[8] hydroboration of $[(H_2C{=}CH)SiRNH]_n$ (R = H, Cl, CH_3)[8] or dehydrocoupling of ammonia[15] or cyanamide[16] with tris(hydridosilylethyl)boranes, $B(C_2H_4SiRH_2)_3$ (R = H, CH_3).[17] NMR investigations suggested that the ceramics, after annealing to temperatures above 1750−1850 °C in a nitrogen atmosphere, are composed of crystalline SiC, Si_3N_4, h-BN, and sp^2-C.[18]

The unusual thermal stability of such compositions is surprising, because thermodynamic calculations by the *CalPhaD* approach[19] on the basis of the elemental composition of the ceramics predict that Si−B−C−N ceramics thermally behave like their boron-free ternary counterparts. Recently several papers have appeared which gave conclusive explanations for the superior thermal stability of Si−B−C−N ceramics derived from boron-modified polysilazanes or polysilylcarbodiimides.[8,9,20,21] It was shown by transition electron microscopy (TEM) that during a post-thermolysis heat treatment the materials developed a special morphology. Both silicon carbide and silicon nitride crystallization was observed. In contrast to ternary Si−C−N ceramics which form micro-composites,[22−24] the quaternary compositions developed morphologies in which nanocrystalline silicon carbide and silicon nitride were embedded in a turbostratic ordered third phase. From electron energy loss spectra (EELS) it was concluded that this turbostratic phase is composed of carbon, boron, and nitrogen.[25,26] Investigations by means of solid-state nuclear magnetic resonance (NMR) suggested that carbon was present as graphite and that boron and nitrogen formed h-BN.[18,27]

It was stated that it is the special arrangement in which the BNC_x phase homogeneously encapsulates silicon nitride nanocrystals which is the key to understanding the extraordinary thermal stability of Si−B−C−N ceramics: carbon (as graphite) is chemically bonded in the BNC_x phase, consequently its activity decreases.[8,26] Because of the encapsulation, nitrogen diffusion (degassing) from the crystals is hindered and the local partial pressure of nitrogen on the internal crystal surfaces can increase significantly.[14a,19] It was calculated thermodynamically that the combination of both effects can be responsible for the thermal stability of the materials.[19]

In contrast to Si−C−N ceramics, which have been studied extensively in recent years (see Part I[1] for a compilation of references), until now, only little is known about the structure of amorphous Si−B−C−N ceramics as-obtained after thermolysis.[28] It is expected that the amorphous state to a significant extent influences the structure of the crystalline composites and thus the thermal properties of the materials.

Whereas Si−C−N ceramics, as studied in Part 1,[1] can be produced over a wide range of compositions, the number of different Si−B−C−N ceramics is still restricted. In the present work three available Si−B−C−N ceramics were investigated which were derived from $[^{11}B(C_2H_4SiR{-}NH)_3]_n$ (R = H, CH_3) obtained on two different reaction pathways. A systematic study of the effect of the precursor source on the composition and microstructure of the amorphous Si−B−C−N ceramics is out of the scope of this investigation. The short-range and medium-range order of the Si−B−C−N ceramics is investigated by means of X-ray and neutron scattering in the wide-angle and small-angle regimes and compared with those of related Si−C−N ceramics. It is the aim of these experiments to contribute toward a better understanding of the phase evolution and the unusual high-temperature properties of Si−B−C−N ceramics.

2. Experimental Section

2.1. Samples. The Si−B−C−N ceramics C1−C3 were obtained by thermolysis of boron-modified polysilazanes. Boron-modified polysilazanes with comparable molecular structure $[^{11}B(C_2H_4SiR{-}NH)_3]_n$ (R = H, CH_3) which were therefore chosen, were obtained on two different reaction pathways, i.e., cross-linking of a single source precursor (C1) vs modification of polymers (C2, C3). Synthesis was performed in analogy to procedures reported in the literature.[7,8] However, because of

(14) (a) Seifert, H. J. *Thermodynamic calculations and experimental phase analysis of ceramic systems*; Habilitation Thesis, Universität Stuttgart, Germany, 2002. (b) Weinmann, M. *Molecular Precursors for high temperature-stable Si−B−C−N ceramics*; Habilitation Thesis, Universität Stuttgart, Germany, 2003.

(15) Weinmann, M.; Nast, S.; Berger, F.; Müller, K.; Aldinger, F. *Appl. Organomet. Chem.* **2001**, *15*, 867.

(16) Weinmann, M.; Herz, M.; Berger, F.; Müller, A.; Müller, K.; Aldinger, F. *J. Organomet. Chem.* **2002**, *659*, 29.

(17) Weinmann, M.; Kamphowe, T. W.; Fischer, P.; Aldinger, F. *J. Organomet. Chem.* **1999**, *592*, 115.

(18) (a) Schuhmacher, J.; Berger, F.; Weinmann, M.; Bill, J.; Aldinger, F.; Müller, K. *Appl. Organomet. Chem.* **2001**, *15*, 809. (b) Schuhmacher, J. *Festkörper-NMR−Untersuchungen zur Umwandlung von Polysilazanen und Polysilylcarbodiimiden in Si−(B)−C−N−Keramiken*; Ph.D. Thesis, University of Stuttgart, Germany, 2000.

(19) (a) Seifert, H. J.; Aldinger, F. *Z. Metallkd.* **1996**, *87*, 841. (b) Seifert, H. J.; Lukas, H.-L.; Aldinger, F. *Ber. Bunsen-Ges. Phys. Chem.* **1998**, *102*, 1309. (c) Peng, J. *Thermochemistry and Constitution of Precursor-Derived Si−(B)−C−N Ceramics*; Ph.D. Thesis, University of Stuttgart, Germany, 2002.

(20) Janakiraman, N.; Weinmann, M.; Aldinger, F.; Schuhmacher, J.; Bill, J.; Singh, P. *J. Am. Ceram. Soc.* **2002**, *85*, 1807.

(21) Bill, J.; Kamphowe, T. W.; Müller, A.; Wichmann, T.; Zern, A.; Jalowieki, A.; Mayer, J.; Weinmann, M.; Schuhmacher, J.; Müller, K.; Peng, J. Q.; Seifert, H. J.; Aldinger, F. *Appl. Organomet. Chem* **2001**, *15*, 777.

(22) (a) Kleebe, H. J.; Suttor, D.; Müller, H.; Ziegler, G. *J. Am. Ceram. Soc.* **1998**, *81*, 2971. (b) Müller, H.; Kleebe, H.-J.; Suttor, D.; Ziegler, G. *Key Eng. Mater.* **1997**, *132−136*, 2005. (c) Trassl, S.; Suttor, D.; Motz, G.; Rössler, E.; Ziegler, G. *J. Eur. Ceram. Soc.* **2000**, *20*, 215.

(23) (a) Bill, J.; Seitz, J.; Thurn, G.; Dürr, J.; Canel, J.; Janos, B.; Jalowiecki, A.; Sauter, D.; Schempp, S.; Lamparter, H.-P.; Mayer, J.; Aldinger, F. *Phys. Status Solidi A* **1998**, *166*, 269. (b) Bill, J.; Schuhmacher, J.; Müller, K.; Schempp, S.; Seitz, J.; Dürr, J.; Lamparter, H. P.; Golczewski, J.; Peng, J.; Seifert, H. J.; Aldinger, F. *Z. Metallkd.* **2000**, *91*, 335.

(24) Weinmann, M.; Zern, A.; Aldinger, F. *Adv. Mater.* **2001**, *13*, 1704.

(25) (a) Jalowiecki, A.; Bill, J.; Aldinger, F.; Mayer, J. *J. Composites* **1996**, *27 A*, 717. (b) Jalowiecki, A.; Bill, J.; Mayer, J.; Aldinger, F. *Proc. Werkstoffwoche, Symp. 7 München (Germany)*, 1996. In Materialwissenschaftliche Grundlagen, F. Aldinger, H. Mughrabi, Eds.; DGM-Informationsgesellschaftlicher Verlag, Frankfurt 657-662 (1997).

(26) Wichmann, T. *Erzeugung innerer Grenzflächen durch in- situ-Kristallisation amorpher anorganischer Festkörper*; Ph.D. Thesis, University of Stuttgart, Germany, 2001.

(27) Jeschke, G.; Kroschel, M.; Jansen, M. *J. Non-Cryst. Solids* **1999**, *260*, 216.

(28) Baldus, H.-P.; Jansen, M.; Sporn, D. *Science* **1999**, *285*, 699.

Table 1. Details on the Synthesis of the Precursors for C1−C3[a]

	scale	polymer comp. found (calc.)	product yield (%)	ceramic yield (%)[b]
C1	12.5 g $^{11}B(C_2H_4Si(CH_3)Cl_2)_3$; excess ammonia; 500 mL THF	$Si_3B_{1.0}C_{9.4}N_{2.8}H_{25}$ ($Si_3B_{1.0}C_9N_3H_{24}$)	70	51
C2	42.5 g $[(H_2C{=}CH)Si(CH_3){-}NH]_n$; 19.6 g $^{11}BH_3{\cdot}NEt_3$; 800 mL toluene	$Si_3B_{1.0}C_{9.1}N_3H_{23}$ ($Si_3B_{1.0}C_9N_3H_{24}$)	100	56
C3	37.2 g $[(H_2C{=}CH)SiH{-}NH]_n$; 19.6 g $^{11}BH_3{\cdot}NEt_3$; 800 mL toluene	$Si_3B_{1.1}C_{6.2}N_{3.2}H_{18}$ ($Si_3B_{1.0}C_6N_3H_{18}$)	100	86

[a] For further details please see refs. 7, 8, and 29. [b] Determined by thermogravimetric analysis (TGA) in an argon atmosphere (T:25−1400 °C, heating rate 2 °C/min).

the high neutron absorption cross section of natural boron it was necessary to prepare the Si−B−C−N ceramics with the isotope ^{11}B and the synthetic approaches were slightly modified. Instead of $^{nat}BH_3{\cdot}SMe_2$ which is commercially available, $^{11}BH_3{\cdot}NEt_3$ was used as a hydroborating reagent. Details on the stoichiometries used, product yields, and ceramic yields are given in Table 1.

Synthesis of the precursor for C1 proceeded as follows.

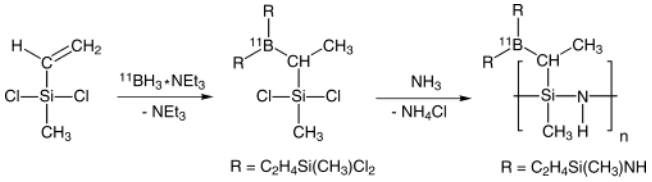

According to the procedure described by Riedel et al.,[7] C1 precursor was obtained by a hydroboration reaction of $(H_2C{=}CH)Si(CH_3)Cl_2$ using $^{11}BH_3{\cdot}NEt_3$ in toluene solution and subsequent ammonolysis in THF. $^{11}BH_3{\cdot}NEt_3$ was synthesized in a two step reaction from $^{11}B(OH)_3$ via $^{11}B(OMe)_3$ and subsequent treatment with $LiAlH_4$.[30] The hydroboration was performed in toluene solution by dropwise addition of the borane to the chlorovinylsilane and the reaction temperature controlled not to exceed 25 °C. Following this, all volatile parts were evaporated in a high vacuum at 25 °C. The residue was dissolved in tetrahydrofuran and the solution was cooled to 0 °C. Under vigorous stirring, a moderate stream of ammonia was introduced to the solution whereby ammonium chloride precipitation was observed immediately. Ammonia addition was continued until liquid ammonia condensed at the reflux condenser which was attached to the reaction tube and which was cooled to −70 °C. After the reaction mixture was warmed overnight to 25 °C, the precipitate was removed by filtration through Celite and the solvent was removed in a high vacuum to produce $[^{11}B(C_2H_4Si(CH_3){-}NH)_3]_n$ as an air- and moisture-sensitive colorless powder.

Synthesis of the precursors for C2 and C3 proceeded as follows.

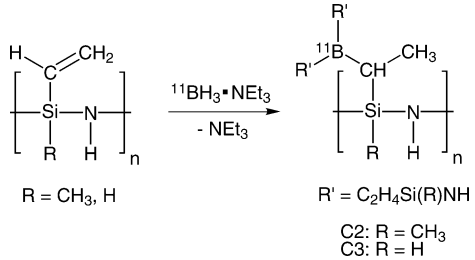

C2 and C3[8] precursors were obtained by a hydroboration reaction of $[(H_2C{=}CH)Si(CH_3){-}NH]_n$[31] and $[(H_2C{=}CH)SiH{-}NH]_n$,[32] respectively, using $^{11}BH_3{\cdot}NEt_3$ as a borane source. The polysilazanes were dissolved in toluene, and the solution of $^{11}BH_3{\cdot}NEt_3$ in toluene was added quickly. During the slightly exothermic reaction the mixture was cooled in a water bath, and the temperature was controlled to not rise above 40 °C. In the case of the synthesis of $[^{11}B(C_2H_4SiH{-}NH)_3]_n$ (precursor for C3) the reaction mixture gelled within approximately 2 h to form a colorless rubber-like gel. In contrast, no significant increase in viscosity of the reaction solution was observed in the synthesis of $[^{11}B(C_2H_4Si(CH_3){-}NH)_3]_n$ even after 12 h. After removing the solvent and volatile compounds in a high vacuum at finally 70 °C, both precursors were obtained as colorless powders.

Table 2. Chemical Composition and Atomic Density ρ_0 of the Si−B−C−N Ceramics C1−C3 and of the Si−C−N Ceramic A2

sample	heat treatment (°C)	c_{Si} (at. %)	c_B (at. %)	c_C (at. %)	c_N (at. %)	ρ_0 (Å^{-3})
C1	1400	23.9	10.1	41.0	25.0	0.077
C2	1400	25.5	7.1	42.4	25.0	0.079
C2	1600	29.1	8.3	45.8	16.8	0.087
C2	1700	28.6	8.6	48.6	14.2	0.088
C3	1400	23.8	8.7	42.5	25.0	0.083
A2	1050	27.8		44.9	27.3	0.075
A2	1400	31.3		38.0	30.7	0.079

Bulk ceramization of all polymers was performed in alumina Schlenk tubes in an atmosphere of flowing Ar. Because of their sensitivity toward oxygen and moisture if not fully thermolyzed (Si−B−C−N ceramics frequently contain a significant amount of hydrogen, i.e., 1−2 mass-%, if thermolyzed only at 1050 °C), thermolysis of the precursors was performed at 25−1400 °C (heating rate 1 °C/min, additional dwell time at the final temperature 3 h) to deliver amorphous ceramics with a slight metallic gloss. For a further heat treatment, as-obtained materials were annealed in a nitrogen atmosphere in graphite furnaces using graphite crucibles (T < 1400 °C, 10 °C/min; T > 1400 °C, 2 °C/min).

The chemical compositions and atomic densities of the investigated precursor-derived Si−B−C−N ceramics C1−C3 are listed in Table 2.

2.2. Diffraction Experiments and Data Evaluation. The diffraction experiments with the amorphous ceramics and the data correction procedures were performed as described for the Si−C−N ceramics in Part I.[1] In addition, the high-temperature behavior of the Si−B−C−N ceramics was investigated by X-ray diffraction using a $\theta-\theta$ diffractometer (Philips XPert MPD) in Bragg−Brentano geometry with Cu Kα radiation.

3. Results and Discussion

The theoretical background of wide-angle and small-angle scattering, as far as relevant for this study, is described in Part I.[1]

3.1. Wide-Angle Scattering. *3.1.1. Total Structure Factors.* Figure 1 shows the structure factors $S(q)$

(29) Haug, J. *Untersuchung der Struktur und des Kristallisationsverhaltens von Si−C−N− und Si−B−C−N−Precursorkeramiken mit Röntgen- und Neutronenbeugung*; Ph.D. Thesis, University of Stuttgart, Germany, 2002.

(30) Nöth, H. Personal Communication.

(31) Choong Kwet Yive, N. S.; Corriu, R. J.; Leclercq, D.; Mutin, P. H.; Vioux, A. *Chem. Mater.* **1992**, *4*, 141.

(32) Choong Kwet Yive, N. S.; Corriu, R. J.; Leclercq, D.; Mutin, P. H.; Vioux, A. *New J. Chem.* **1991**, *15*, 85.

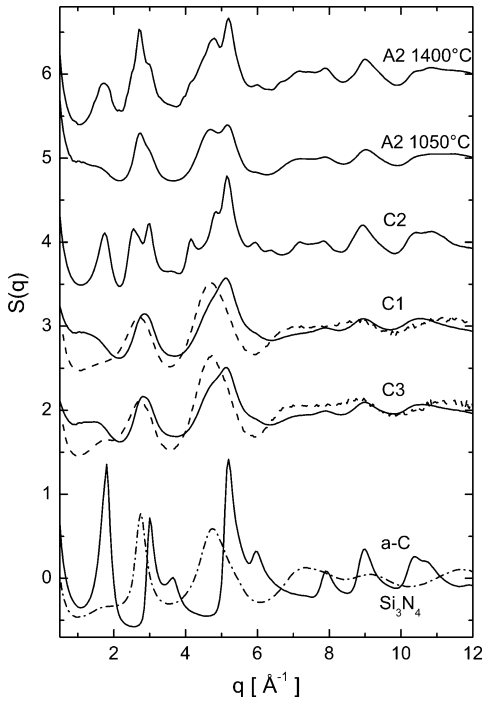

Figure 1. Total neutron (—) and X-ray (– – –) structure factors $S(q)$ of the amorphous Si−B−C−N ceramics C1−C3, of the Si−C−N ceramic A2 at 1050 °C and 1400 °C, and of amorphous carbon (a-C) (—) and amorphous Si_3N_4 (– · –).

obtained from neutron diffraction (—) of the amorphous Si−B−C−N ceramics C1−C3 thermolyzed at 1400 °C and of the ceramics C1 and C3 obtained from X-ray diffraction (– – –). In contrast to the pyrolysis of boron-free polysilazanes, higher thermolysis temperatures, i.e., 1400 °C, were required to fully transform the boron-containing precursors into ceramic materials. The reason for that is that residual hydrogen remains in the materials if only heated to 1050 °C. It causes a distinct sensitivity of the ceramics toward hydrolysis and/or oxidation if exposed to air.

For a comparison, the structure factors of a Si−C−N ceramic (A2, derived from $[(H_2C{=}CH)Si(CH_3)NH]_n$; the composition of this material is located within the three-phase field C/SiC/Si_3N_4[1]) thermolyzed at 1050 °C and annealed for 16 h at 1400 °C are represented. The bottom curves in the figure correspond to the structure factors of amorphous carbon (—) and amorphous Si_3N_4 (– · –) (from Part I[1]). Apparently, the addition of boron does not significantly modify the general features of the structure factor of the ceramics (cf. A2 and C1 in Figure 1). The comparison of the structure factors of the ceramics with those of a-C and a-Si_3N_4 suggests that the structure factors are composed of these two $S(q)$ functions. This was already found for Si−C−N ceramics discussed in Part I and was interpreted by a separation of the ceramic into two amorphous phases: an amorphous $Si_{3+(1/4)x}C_xN_{4-x}$ phase and an amorphous graphite-like phase.

The contrast between X-ray and neutron diffraction is due to the different weighting of the contributions of these two phases: with X-rays the contribution of the amorphous Si_3N_4 phase is clearly visible (see, e.g., the peak at $q \approx 4.8$ Å^{-1}), whereas with neutrons the contribution of amorphous carbon is more emphasized (see, e.g., the peaks at $q \approx 1.5$ Å^{-1} and 5.1 Å^{-1}).

In the case of the Si−C−N ceramics, additional annealing after thermolysis caused a coarsening of the two separated phases a-Si_3N_4 and a-C. This led to a more pronounced split of the peaks at $q \approx 3$ Å^{-1} and $q \approx 5$ Å^{-1}, and a sharpening and shift to higher q-values of the peak at $q \approx 1.5$ Å^{-1} corresponding to an increase of the order between the hexagonal planes in a-C (cf. A2 in Figure 1). Comparison with Si−B−C−N ceramics C1 and C3, thermolyzed at 1400 °C, shows that they possess features similar to those of Si−C−N ceramics thermolyzed at 1050 °C. Even though heat-treated at higher temperature, the split of the peaks is even less pronounced than that for A2. This indicates that the addition of about 10 at. % of boron to the ceramics causes a delay of the coarsening of the two separated amorphous phases and of the structural change of the a-C phase. This is in agreement with findings published recently by Müller et al.[33] They investigated in detail the influence of various amounts of boron on the thermal stability of Si−B−C−N ceramics using TGA and XRD. It turned out that, depending on the molecular structure of the precursor, approximately 7−9 at. % of B are required to efficiently prevent the ceramics from decomposition and early crystallization.

The Si−B−C−N ceramic C2 in Figure 1 exhibits a much more pronounced splitting of the peaks than the ceramics C1 and C3, indicating that the thermolysis of this sample at 1400 °C led to a more advanced state of phase separation, comparable to that of the Si−C−N ceramic A2 after annealing at 1400 °C/16 h. Noting that the ceramic C2 does not show improved high-temperature stability compared to Si−C−N ceramics (see section 3.1.4, below) it can be concluded that this property is closely connected with the hindered kinetics of the growth of the separated phases, already below the crystallization temperature. The reason for the different behavior of C1 and C3 on one hand and C2 on the other hand is not yet understood in detail. However, demixing during thermolysis of C2 might be a consequence of the reaction pathway used in combination with the molecular structure of the polymer. It was stated[6] that cross-linking of single-source precursors (such as in the synthesis of C1) delivers polymers with a more homogeneous distribution of the constituting elements than modification of polymers, e.g., by hydroboration (of polysilazanes, synthesis of C2, C3). The reason for the difference in the properties of C2 and C3 can only be hypothesized. Most probably differences in the chemistry during thermolysis are responsible. $[^{11}B(C_2H_4SiH{-}NH)_3]_n$ (precursor for C3) exhibits Si−H and N−H units which undergo dehydrogenative cross-linking reactions below 250 °C. Hereby Si−N bonds form, releasing SiN_3C structural units.[8,14b] With increasing temperature (500 °C), a second important reaction takes place. B−N and Si−C bonds form at the expense of B−C and Si−N bonds.[8,14b,18] Consequently, SiN_2C_2 environments are generated. The pyrolysis chemistry of C2 is more complex. Because it does not possess latent reactivity, i.e., the ability to further cross-link at low temperature, thermolysis is to a significant portion characterized by depolymerization reactions and volatilization of low-

(33) (a) Müller, A.; Gerstel, P.; Weinmann, M.; Bill, J.; Aldinger, F. *J. Eur. Ceram. Soc.* **2001**, *21*, 2171. (b) Müller, A.; Gerstel, P.; Weinmann, M.; Bill, J.; Aldinger, F. *J. Eur. Ceram. Soc.* **2000**, *20*, 2655.

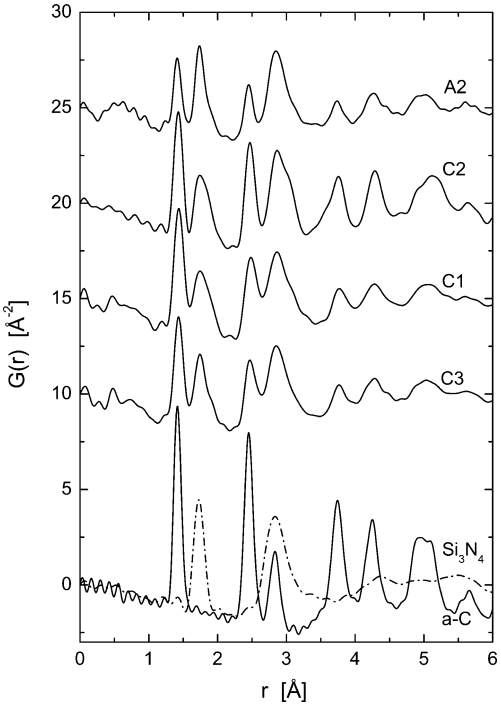

Figure 2. Total neutron pair correlation functions $G(r)$ of the amorphous Si−B−C−N ceramics C1−C3, of the Si−C−N ceramic A2 (derived from $[(H_2C{=}CH)Si(CH_3)NH]_n$ after thermolysis at 1050 °C[1]), and of amorphous carbon (a-C) (—) and amorphous Si_3N_4 (– · –).

molecular-weight species. Consequently, a ceramic material is released with less homogeneous distribution of the constituting elements than C3. The differences in the atomic rearrangement during thermolysis are, for example, reflected in the NMR spectra of thermolysis intermediates. Whereas in the ^{29}Si NMR spectrum of C2 after a heat treatment to 400 °C at least four different resonance signals, which cannot be assigned unequivocally, can be distinguished, the respective spectrum of C3 exhibits only three signals centered at −4, −15, and −37 ppm which can be attributed to SiN_2C_2, SiN_2HC, and SiN_3C sites, respectively.[18]

In conclusion of this section it has to be stated that the questions concerning the effects of the precursor source and of the reaction pathway on the structure of the final Si−B−C−N ceramics cannot be answered on the basis of only three investigated examples. Ceramics C1 (from single-source precursor) and C3 (from modifying of a polymer) exhibit practically identical structure factors, whereas the behavior of C2 (obtained by modification of a polymer) is different. Hence, further extensive investigations of a variety of Si−B−C−N ceramics are needed to clarify these questions.

3.1.2. Total Pair Correlation Functions. The total neutron pair correlation functions $G(r)$ of the Si−B−C−N ceramics C1−C3 and of the Si−C−N ceramic A2 are shown in Figure 2. Comparison of the $G(r)$-functions shows that the addition of boron does not cause an obvious change of the order, the general structural features of the Si−B−C−N ceramics are the same as those already found for the Si−C−N ceramics (Part I[1]). With neutron scattering four peaks in the range up to 3 Å are found which correspond well with the distances in crystalline Si_3N_4 and graphite, respectively (see Table 3). Those at 1.74 and 2.87 Å which belong to the Si−N and N−N distances in Si_3N_4 show an additional shoulder at greater distances, indicating additional Si−C bonds in mixed $Si(C,N)_4$ tetrahedra (see Part I[1] for details). Thus, it can be concluded from the $G(r)$ of the Si−B−C−N ceramics (in the same way as has been done for the Si−C−N ceramics) that they are separated into two phases: amorphous $Si_{3+(1/4)x}C_xN_{4-x}$ and an amorphous graphite-like phase.

We note that the differences between Si−C−N ceramics A2 and Si−B−C−N ceramics C1−C3, and also those between C2 and C1, C3 are much more evident in the structure factors $S(q)$ (Figure 1) than in the pair correlation functions $G(r)$ (Figure 2). This indicates that the atomic short-range order of the different ceramics (displayed by the first few peaks in $G(r)$) is much the same, whereas the intermediate-range order, in the present case the stage of phase-separation and the order between the planes of the graphite-like phase (affecting the first peaks in $S(q)$), is different.

3.1.3. Incorporation of Boron Atoms. From more detailed investigations of the pair correlation functions of Si−B−C−N ceramics, differences relative to those of the Si−C−N ceramics were discovered. Figure 3 shows the pair correlation functions of the Si−B−C−N ceramic C1 (—) and of the Si−C−N ceramic A2 (– – –) with comparable Si/C/N ratio obtained by neutron scattering. The peaks at $r_1 = 1.42$ Å and at $r_2 = 2.46$ Å in Si−C−N ceramics, which are assigned to C−C correlations, are shifted to higher r-values for the Si−B−C−N ceramics, $r_1 = 1.44$ Å and $r_2 = 2.48$ Å (here the numbering of the peaks refers to those belonging to the graphite-like phase). A comparison of these values with those of graphite, $r_1 = 1.42$ Å, $r_2 = 2.46$ Å, and hexagonal boron nitride $r_1 = 1.46$ Å, $r_2 = 2.50$ Å, indicates that the atomic distances in Si−B−C−N ceramics lie between these two phases. Further, the area below the peaks is larger for the Si−B−C−N ceramics than for the Si−C−N ceramics. The analysis of the coordination numbers results in physically meaningful values only if two contributions, C−C and B−N bonds, to the peaks at r_1 and r_2, respectively, are taken into account (considering only a C−C contribution for the peak at r_1 resulted in a coordination number larger than 3).[29]

The conclusion drawn from atomic distances and evaluation of coordination number is that the boron atoms in the Si−B−C−N ceramics are incorporated in a structure with hexagonal short-range order. For this BNC phase three possibilities can be discussed: (i) the different atomic species are arranged randomly in mixed rings, (ii) the layers consist of BN and C rings, and (iii) there exist alternating BN and C layers. To argue the different aspects the local expansion of the hexagonal rings as a consequence of B−N bonds is investigated. The local expansion is characterized (for a coordination shell, n, by the ratio $V_n = r_n^{SiBCN}/r_n^{SiCN}$ of the distances in the graphite-like phase in Si−B−C−N and Si−C−N ceramics (Figure 4). (The peak r_3 is not taken into account for this consideration because of an overlap with N−N correlations from a-Si_3N_4.) V_n (>1) decreases distinctly between the second and the fourth coordination shell. This means that the B−N bonds giving rise to the expansion exist only within a restricted correlation range, in contrast to the C−C bonds. Thus the case (i) a random distribution of the C, B, and N atoms, can

Table 3. Peak Positions r_{ij} in $G(r)$ for the Si−B−C−N Ceramics C1−C3 and Atomic Distances in Relevant Crystalline Phases, Graphite,[34] h-BN,[35] α-Si_3N_4,[36] and SiC[37]

material	peak position r_{ij} (Å) (atomic pair ij)					
C1	1.44	1.74	1.91	2.48	2.87	3.11
C2	1.43	1.74	1.88	2.48	2.87	3.08
C3	1.44	1.75	1.92	2.48	2.86	3.14
	(C−C)			(C−C)	(C−C)	
	(B−N)			(B−B, N−N)	(B−N)	
		(Si−N)		(N−N)	(N−N)	(Si−Si)
			(Si−C)			(Si−Si, C−C)
graphite	1.42			2.46	2.84	
	C−C			C−C	C−C	
h-BN	1.46			2.50	2.89	
	B−N			B−B, N−N	B−N	
α-Si_3N_4		1.71, 1.79		2.58	2.81, 2.94	2.72−3.15
		Si−N		N−N	N−N	Si−Si
SiC			1.89			3.06
			Si−C			Si−Si,C−C

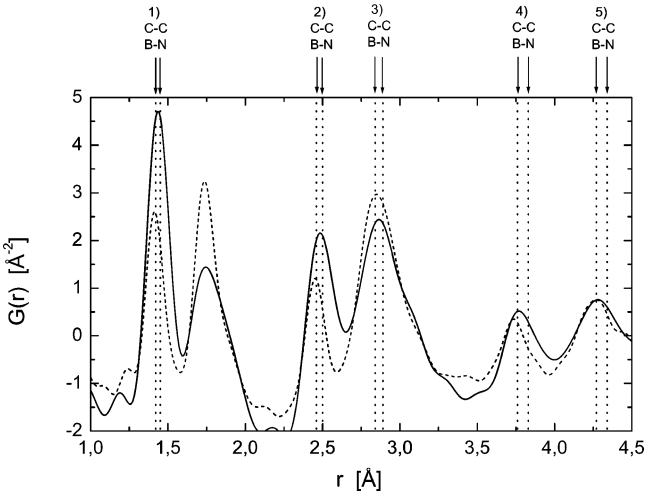

Figure 3. Neutron pair correlation functions $G(r)$ of the Si−B−C−N ceramic C1 (—) and of the Si−C−N ceramic A2 (− − −) after thermolysis at 1400 and 1050 °C, respectively. The addition of boron leads to a shift of the peaks 1−5, which belong to the graphite-like phase, to greater distances. The vertical lines indicate distances in graphite and h-BN.

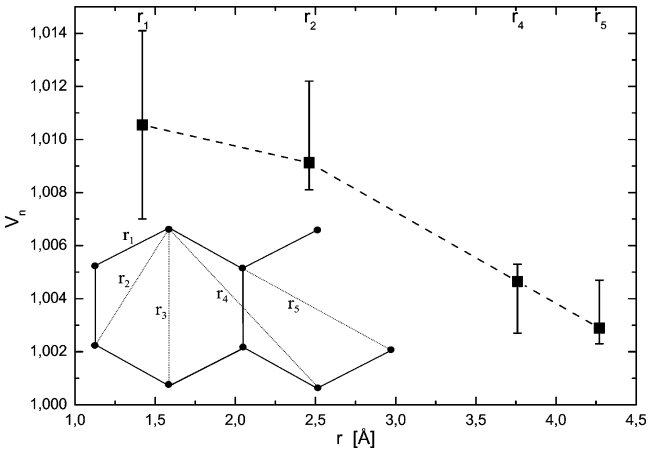

Figure 4. Local expansion of the hexagonal rings as a consequence of B−N bonds characterized by the ratio $V_n = r_n^{SiBCN}/r_n^{SiCN}$ of the distances in the graphite-like phase in Si−B−C−N and Si−C−N ceramics (the dashed line is drawn as guide to the eye). The distances are depicted in the insert. The error bars refer to the spread of the r_n-values from different samples. The distance r_3 cannot be used because of the overlap with contributions from the a-Si_3N_4 phase.

be excluded because this would cause a homogeneous overall expansion of the graphite-like phase with a constant value of V_n. Rather, ranges in this phase formed from BN rings are present which extend only over a few neighboring rings. Accordingly, the expansion $V_n > 1$ is restricted to small distances. At larger distances the correlations only involve carbon atoms forming more extended ranges and V_n therefore approaches the value 1. A distinction between cases (ii) and (iii) is not possible on the basis of the present data. Note that the distances in Figure 4 are in-plane distances; the distance between stacked planes does not give rise to a resolved peak in the $G(r)$-functions, but only to a peak at $q \approx 1.8$ Å^{-1} in the structure factor $S(q)$. A discussion of the distance creating this peak in connection with the addition of boron is not possible because its position strongly depends on the state of relaxation already for the Si−C−N ceramics without boron. In either case, the behavior of the ratio V_n means for case (ii) that small BN regions are embedded in a more extended C plane, and for case (iii) that small BN planes are stacked between more extended C planes. From ^{11}B-MAS NMR spectra it was found likewise that the boron atoms in Si−B−C−N ceramics derived from boron-modified polysilazanes are exclusively surrounded by nitrogen atoms.[18]

3.1.4. High-Temperature Behavior. In this section the phase evolution of the Si−B−C−N ceramic C1, which was found not to thermally degrade below 1850 °C is compared with that of ceramic C2. In contrast to C1, the latter does not withstand such distinct heat treatment. Figure 5 shows a comparison of the X-ray diffraction patterns of the as-thermolyzed samples and after annealing at different temperatures for 16 h.

Ceramic C1 thermolyzed at 1400 °C is fully amorphous (Figure 5a). Additional annealing at 1400 °C for 16 h leads to changes. The broad peak around $2\theta = 23°$ (corresponding to the (002) reflection of graphite) sharpens and shifts to higher 2θ. This effect has also been found for Si−C−N ceramics and was explained with an increase of the order of the stacked hexagonal planes in the graphite-like phase (Part I[1]). In addition, broad diffraction peaks from a nanocrystalline phase appear (at $2\theta = 36°$, 60°, and 72°). From the peak width a crystallite size of about 20 Å was estimated using the Williamson−Hall equation.[38] At higher temperatures these peaks sharpen and increase in intensity, indicating growth of the SiC nano crystals (35 Å at 1500 °C

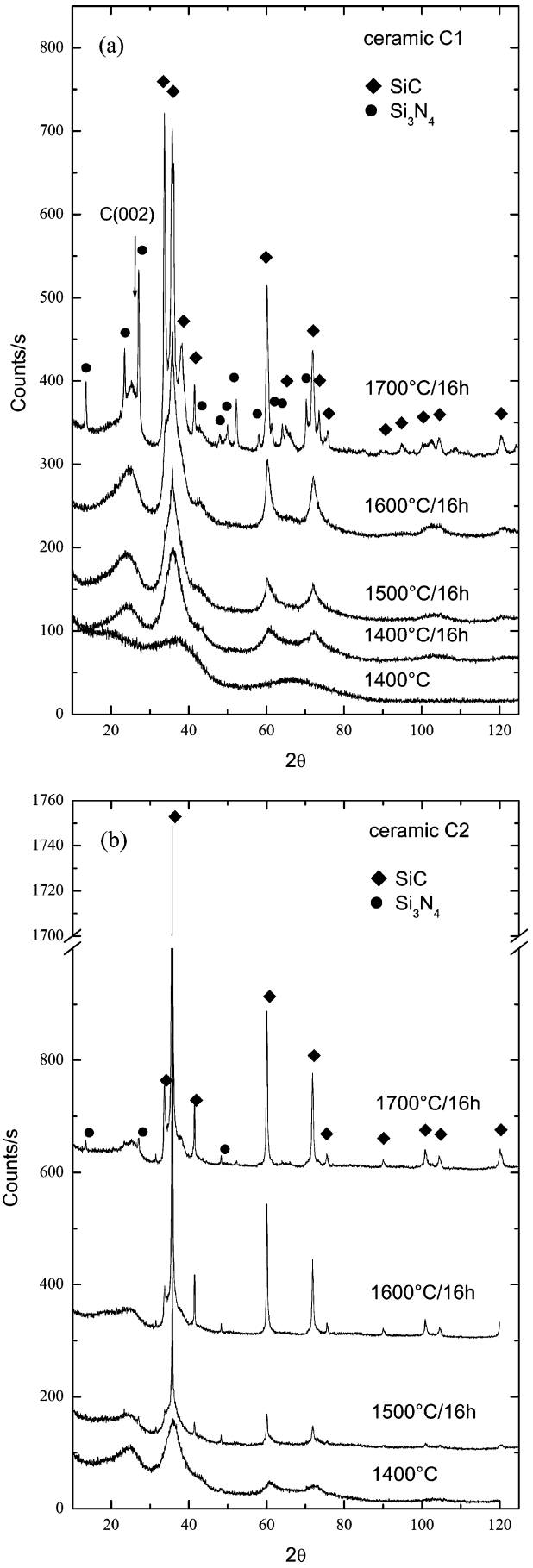

Figure 5. X-ray diffraction (Cu Kα) with Si−B−C−N ceramics C1 (a) and C2 (b) after thermolysis and after annealing for 16 h at different temperatures in 1 bar nitrogen.

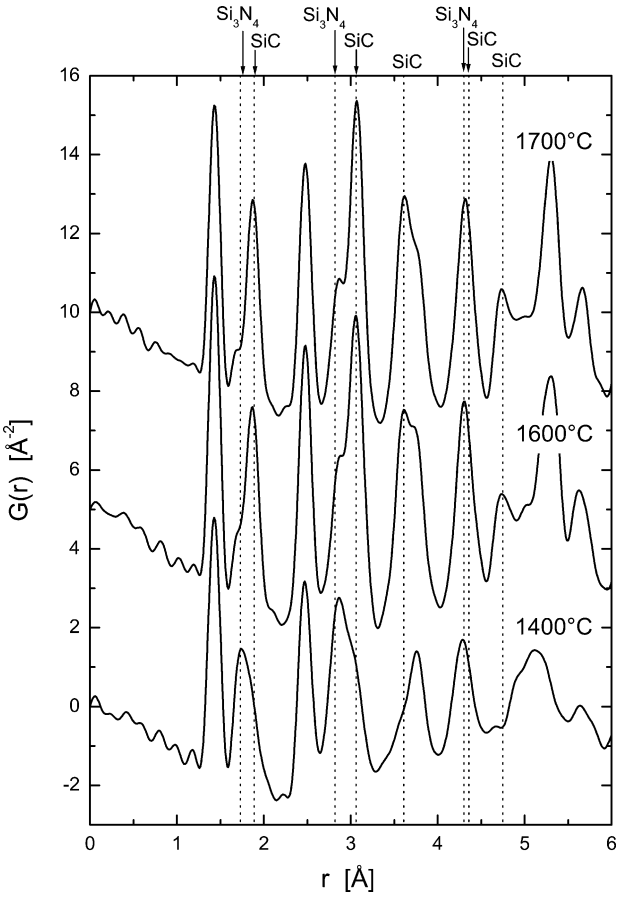

Figure 6. Total neutron pair correlation functions $G(r)$ of the amorphous Si−B−C−N ceramic C2 after thermolysis at 1400 °C and after further annealing at 1600 °C and 1700 °C for 16 h in 1 bar nitrogen.

and 50 Å at 1600 °C). At 1700 °C the amorphous Si_3N_4 phase in the ceramic transforms to crystalline β-Si_3N_4, and accelerated growth of the SiC crystallite occurs. Remarkably, no decomposition of Si_3N_4 according to the reaction

$$Si_3N_4 + 3C \rightarrow 3SiC + 2N_2\uparrow \qquad (1)$$

takes place at this temperature. The phase evolution is different from that of the Si−C−N ceramics reported in Part I[1] where no nanocrystalline SiC phase occurred upon annealing but instead, coarse crystalline Si_3N_4 and SiC, followed by the decomposition of Si_3N_4 at higher temperatures, was observed (for details see ref 29).

The thermal behavior of the Si−B−C−N ceramic C2 is very different from that of ceramic C1 (Figure 5b). The state of the as-thermolyzed sample C2 resembles that of C1 after additional annealing at 1400 °C for 16 h. It contains SiC nanocrystallites with a size of about 30 Å. At 1500 °C the SiC crystallites coarsened significantly, whereas crystalline Si_3N_4 appears only in very small amounts. This points to a decomposition according to the reaction given by eq 1, which is accompanied by a decreasing nitrogen content in ceramic C2 from 25.0 at. % at 1400 °C to 14.2 at. % after annealing for 16 h

(34) Trucano, P.; Chen, R. *Nature* **1975**, *258*, 136.
(35) Pease, R. S. *Acta Crystallogr.* **1952**, *5*, 356.
(36) Ruddlesden, S. N.; Popper, P. *Acta Crystallogr.* **1958**, *11*, 465.
(37) Shaffer, P. T. B. *Acta Crystallogr.* **1969**, *B25*, 477.
(38) Williamson, G. K.; Hall, W. H. *Acta Mater.* **1953**, *1*, 22.

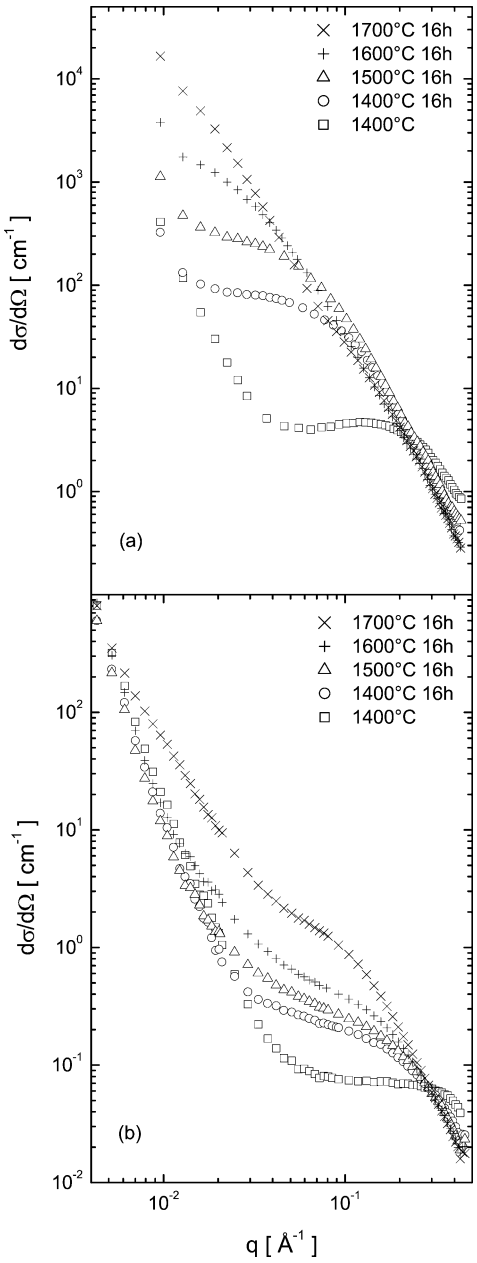

Figure 7. Double logarithmic plot of the small-angle scattering cross sections of the amorphous Si−B−C−N ceramic C1 at thermolysis temperature 1400 °C and after annealing at different temperatures for 16 h in 1 bar nitrogen: (a) X-rays, and (b) neutrons.

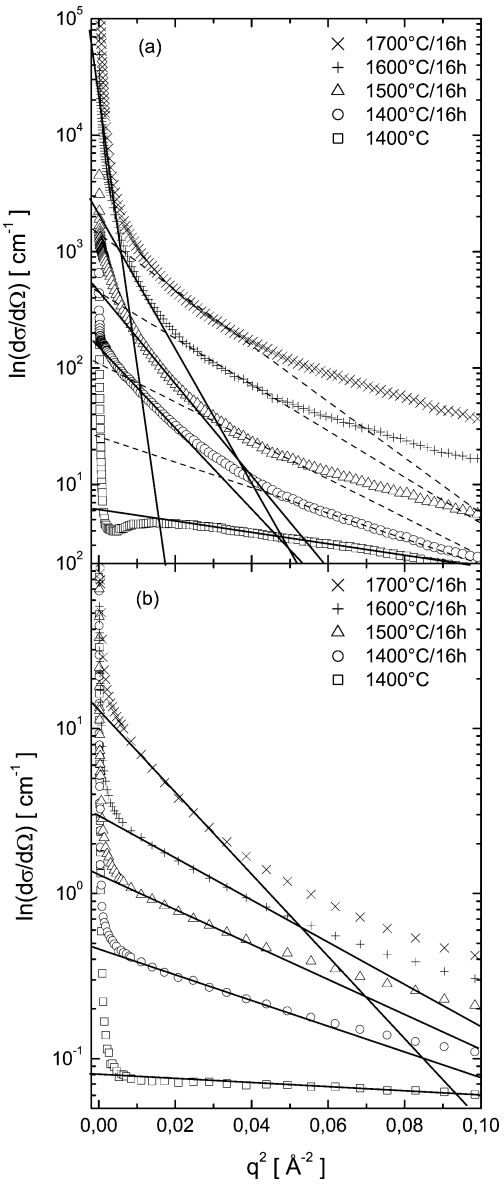

Figure 8. Guinier plots, $\ln(d\sigma/d\Omega)$ versus q^2, for the amorphous Si−B−C−N ceramic C1 at thermolysis temperature 1400 °C and after annealing at different temperatures for 16 h in 1 bar nitrogen: (a) X-rays, and (b) neutrons. The straight lines were fitted to the linear parts in the experimental curves.

at 1700 °C (Table 2). In Figure 6 the pair correlation functions for the ceramic C2 from neutron diffraction at the thermolysis temperature 1400 °C and after further annealing at 1600 and 1700 °C for 16 h are shown. The transition from Si_3N_4 to SiC upon annealing can be assigned clearly: the Si_3N_4 peaks at 1.73 and 2.82 Å vanish, whereas peaks at 1.89 and 3.06 Å appear which can be attributed to Si−C bonds in SiC. In contrast to the amorphous Si−(B)−C−N ceramics, where the only observed distances at 1.89 and 3.06 Å were attributed to mixed $Si(C,N)_4$ tetrahedra, now also greater distances at 3.61, 4.36, and 4.75 Å can be found belonging to the separate crystalline SiC phase.

3.2. Small-Angle Scattering. Figure 7 shows the log−log plots of the normalized small angle neutron and X-ray scattering cross sections of the amorphous Si−B−C−N ceramic C1 thermolyzed at 1400 °C and after further annealing at 1400, 1500, 1600, and 1700 °C for 16 h. It is obvious that the ceramic contains inhomogeneities which cause a signal in the small-angle region already in the as-thermolyzed state. The general features of this scattering effect are quite similar to those observed with the Si−C−N ceramics in Part I:[1] a linear increase toward very small q-values in the log−log plot which is caused by surface scattering from the powder particles according to Porods law[39] followed by

Table 4. Sizes *D* of Inhomogeneities in the Si−B−C−N Ceramic C1 at Different Temperatures from Neutron (*n*) and X-ray (*x*) Scattering[a]

	temperature (°C)				
	1400	1400/16 h	1500/16 h	1600/16 h	1700/16 h
$D(n)$ (Å)	7	18	20	21	34
$D(x)$ (Å)	15	20/39	19/44	21/41	47/93

[a] With X-rays two sizes were detected for the annealed ceramics.

Table 5. Comparison of Calculated Ratio $\Delta\eta_x/\Delta\eta_n$ for X-rays and Neutrons for Possible Regions in a Si−B−C−N Matrix and for a System of Two Separated Phases with the Ratio of the Invariants $(Q_x/Q_n)^{1/2}$ as Determined from the Measured Small-Angle Scattering Cross Sections of Ceramic C1[a]

	$\Delta\eta_x/\Delta\eta_n$				
$(Q_x/Q_n)^{1/2}$	pores in Si−B−C−N	Si_3N_4 in Si−B−C−N	SiC in Si−B−C−N	a-C in Si−B−C−N	$Si_{3+(1/4)x}C_xN_{4-x}$ + BN−C
5.2	3.4	5.4	15	0.74	6.5

[a] The X-ray and neutron scattering lengths were taken from refs 40 and 41. Used number densities for the calculation of the scattering length density η: Si_3N_4, $\rho_0 = 0.103$ Å^{-3}; SiC, $\rho_0 = 0.097$ Å^{-3}; a-C, $\rho_0 = 0.077$ Å^{-3}.

a scattering effect around $q = 0.1$ Å^{-1} from the inhomogeneities in the bulk. The shift of this effect to lower q-values with increasing temperature indicates that the size of the scattering regions is growing with increasing temperature.

The scattering cross sections in Figure 7 show a clear contrast between neutron and X-ray scattering: the cross sections from neutron diffraction being smaller by 1 or 2 orders of magnitude. Additionally, the scattering curves exhibit a different course (except for the thermolyzed samples): the characteristic features in the X-ray scattering curves are shifted to lower q-values which means that in this case inhomogeneities with larger diameters are observed.

The diameter of the scattering regions was determined from the so-called Guinier-plots (Figure 8). If the signal is plotted in a $\ln(I_{coh}(q))$ versus q^2 plot the Guinier radius R_G can be determined from the slope of the linear part of the plot (eq 5 in Part I[1]). Assuming that the scattering regions have a spherical shape the diameter D can be calculated as $D = 2\cdot\sqrt{5/3}\cdot R_G$. The results are listed in Table 4. For the X-ray curves two linear parts can be fitted corresponding to two sizes of scattering regions. The values of the smaller inhomogeneities correspond to the values as obtained by neutron scattering. The size of these smaller regions increases with increasing temperature from $D \approx 10$ Å after thermolysis at 1400 °C up to $D \approx 40$ Å at 1700 °C/16 h. The size of the larger inhomogeneities which were only observed with X-ray scattering (and only for the annealed samples) grows from $D \approx 40$ Å at 1400 °C/16 h up to $D \approx 90$ Å at 1700 °C/16 h. These values for the larger regions correspond fairly well to the size of SiC nanocrystallites found in the crystallization experiments (Section 3.1.4).

For the identification of the inhomogeneities, contrast variation between X-rays and neutrons was employed, adopting the same method as described in Part I.[1] The ratios $\Delta\eta_x/\Delta\eta_n$ of the difference of the scattering length densities $\Delta\eta$ between scattering regions and matrix for X-rays and neutrons are calculated for different types of inhomogeneities, i.e., for possible regions in a matrix and for a system of two separated phases, and are compared with the ratio of the invariants $(Q_x/Q_n)^{1/2}$ as determined from the measured small-angle scattering cross sections. The values are given in Table 5 for the as-thermolyzed ceramic C1. The results of these calculations show good agreement for the case of a system of two separated phases of amorphous $Si_{3+(1/4)x}C_xN_{4-x}$ and of amorphous graphite-like BN−C which is a verification of the results from the wide-angle scattering investigations. The case of an amorphous Si_3N_4 phase segregated in an amorphous Si−B−C−N matrix, showing comparable agreement in Table 5, can be excluded on the basis of the wide-angle results.

The contribution of pores to the small-angle scattering signal cannot be excluded on the basis of the data in Table 5 alone. However in an extensive study on Si−C−N ceramics[42] it has been demonstrated that modeling of the shape of the measured small-angle scattering curves assuming pores as scattering regions was not possible, because in this case a very low volume fraction of pores had to be introduced which did not give rise to the observed interference effect around $q = 0.1$ Å^{-1}. Furthermore, the application of the immersion technique[29] proved that this scattering effect is not influenced by surface scattering effects, whereas in the case of pores part of them should be located at the surfaces of the powder particles, i.e., not closed, and thus should be detectable by the immersion technique. From these observations it has been concluded that internal porosity, which is common in precursor-derived ceramics, occurs on a larger size scale than probed by the small-angle scattering window around $q = 0.1$ Å^{-1}. This porosity then contributes to the Porod scattering at very small q values (see above).

In annealed ceramic C1 nanocrystalline SiC regions are present in addition to the two separated amorphous phases (Section 3.1.4). Therefore, the discussion of the contrast between X-rays and neutrons in the same way is not possible. However, the large value of the ratio $\Delta\eta_x/\Delta\eta_n$ of about 15 explains why the SiC nanocrystals are detected only by X-rays in the small-angle scattering curves.

Comparison of the small-angle neutron scattering curves for the Si−B−C−N ceramic (Figure 7b) and for the Si−C−N ceramics (Part I[1], Figure 8) shows that comparable curves are found at temperatures which are about 200 K higher for the boron-containing ceramics. Thus, the hindering of the coarsening of the separated phases in the ceramics upon addition of boron, as revealed by the investigation of the short-range order (Section 3.1) is confirmed by the small-angle scattering results.

Conclusions

The atomic short-range order in precursor-derived Si−B−C−N ceramics (containing up to 10 at. % boron) corresponds to that in Si−C−N ceramics. The Si−B−C−N ceramics are separated into two phases:

(39) Porod, G. *Kolloid Z.* **1951**, *124*, 83.

(40) Hubbell, J. H.; Veigele, W. J.; Briggs, E. A.; Brown, R. T.; Cromer, D. T.; Howerton, R. J. *J. Phys. Chem. Ref. Data* **1975**, *4*, 471.

(41) Sears, V. F. *Neutron News.* **1992**, *3*, 26. (Taylor & Francis Journals, ISSN 1044-8632)

(42) Schempp, S. *Untersuchung des Relaxationsverhaltens amorpher Si−C−N Keramiken bei thermischer Behandlung mit Hilfe der Röntgen- und Neutronenkleinwinkelstreuung*; Ph.D. Thesis, UniversitΣt Stuttgart, 1998.

amorphous $Si_{3+(1/4)x}C_xN_{4-x}$ and an amorphous graphite-like phase, already after thermolysis, on a size scale of the order of 10 Å. The boron atoms are bond exclusively to N and are incorporated in the graphite-like phase. Thus, the latter actually consists of BN- and C-rings. The regions formed by BN-rings are less extended than those formed by C-rings.

By addition of boron atoms to Si−C−N ceramics the kinetics of the coarsening process of the separated amorphous phases upon additional annealing change.

In contrast to the Si−C−N ceramics, annealing of Si−B−C−N ceramics causes the development of nanocrystalline SiC and of Si_3N_4. Moreover the decomposition of the Si_3N_3 by reaction with carbon occurs at significantly higher temperatures.

Acknowledgment. This work was supported by the Deutsche Forschungsgemeinschaft through grant La 686/3-2. The help of Dr. Luec Auvray (LLB, Saclay, France) during the neutron small-angle diffraction experiments and of Dr. Chris Benmore (ISIS, Didcot, UK) during the neutron wide-angle diffraction experiments is highly appreciated.

CM031088T